Supplementary Information (SI) for Inorganic Chemistry Frontiers.

Supporting Information

Intensified Ion-to-Channel Interaction within Pyridinic Covalent Organic Framework Membranes towards Exclusive Lithium-ion Sieving

Weihao Yu,[1] Yijun Qian,[2*] Haoqing Ji,[1] Zebin Zhu,[1] Tong Wu,[1] Tao Qian,[2] Chenglin Yan,[2,3*] Jianmei Lu,[1*]

Materials and methods

Chemicals and Materials: 2,4,6-trihydroxybenzene-1,3,5-tricarbaldehyde (Tp, 98%) and 2,5-Diaminopyridine (Py, 97%) were purchased from Jilin Chinese Academy of Sciences-Yanshen Technology Co., Ltd. p-Phenylenediamine (Pa, ≥ 99.0%, GC) and p-Toluenesulfonic acid monohydrate (TsOH, ≥ 98.5%, AR) were purchased from Shanghai Aladdin Biochemical Technology Co., Ltd. Dichloromethane (DCM, ≥ 99.5%, AR) were purchased from Energy Chemical Company. Polyacrylonitrile (PAN) ultrafiltration membranes as the substrate were purchased from Shandong Megavision Membrane Technology & Engineering Co., Ltd., China, and used as received. The following salts and chemicals were used in the iontophoresis test: lithium chloride (LiCl, 99.9% metals basis), nickel chloride, hexahydrate ($NiCl_2 \cdot 6H_2O$, 97%), cobalt chloride, hexahydrate ($CoCl_2 \cdot 6H_2O$, ACS reagent, 98%) and manganese chloride, tetrahydrate ($MnCl_2 \cdot 4H_2O$, ≥ 99% AR) were purchased from Shanghai Aladdin Biochemical Technology Co., Ltd.

Characterizations: SEM (Hitachi SU8010) and high-resolution aberration-corrected transmission electron microscope (Titan Themis Cubed G2 300) technique were used to measure the morphology and thickness of the COF membranes. X-ray diffraction (Bruker D8 advance) measurements in the 2θ range from 2 ° to 40 ° for 2D COF membranes and their corresponding powders synthesized by Pyrex tube strategy (with a step size of 0.02 ° and recording rate of 150 ms) were performed using an Xpert Powder with Cu Kα radiation (λ = 1.5406 Å). FTIR-ATR (Bruker Vertex 70 FTIR) technique was performed to determine the chemical bonding of 2D COFs. XPS (Kratos Axis Ultra Dld, Japan) was used to verify the interaction between cations and COF membranes. Zeta-potential tests of 2D COF membranes were performed using the Solid Surface Zeta Potential Tester (SurPASS 3, Anton Paar, Ltd). Pore size distribution and surface area of 2D COF membranes were characterized by an automatic microporous physical adsorption instrument (Tristar II 3020, Micromeritics, USA) and examined by measuring the N_2 adsorption−desorption isotherm at 77 K in a liquid nitrogen bath.

Fabrication of 2D COF membranes: The defect-free 2D COF membranes were synthesized on the PAN substrates via a contra-diffusion strategy. The PAN substrate was vertically clamped in the middle of a homemade H-shaped electrolytic cell. Typically, 0.2 mmol 1,3,5-triformylphloroglucinol (Tp) was dissolved in a dichloromethane (DCM) solution and filled the chamber facing the PAN side. Then, 0.3 mmol diamine monomer (p-phenylenediamine (Pa) or 2,5-diaminopyridine (Py)) together with 0.6 mmol p-toluenesulfonic acid (TsOH) were dissolved in deionized water and place in another chamber. After leaving the reaction without any disturbance at room temperature for 3 days, the colored 2D COF layers fully covered the face of the PAN substrate, in which the 2D COF-Py film was dark purple, and the 2D COF-Pa film was reddish-brown. Finally, the synthesized 2D COF membranes were washed with ethanol several times and dried at room temperature for further usage.

Fabrication of 2D COF-Py powders: 1,3,5-triformylphloroglucinol (Tp) (0.3 mmol), and 2,5-diaminopyridine (Py) (0.45 mmol) were dissolved in 3 mL (3:1) solvent mixture of dimethylacetamide and o-dichlorobenzene with 0.6 mL of 6 M acetic acid and added to a Pyrex tube (o.d. × i.d. = 10×8 mm^2 and length 18 cm). This mixture was sonicated for 10 min to obtain a homogeneous dispersion, then dissolved after freezing at 77 K (liquid N_2 bath) and cycled three times for degassing. The tube was sealed off and heated at 120 °C for 72 h. A dark purple precipitate was collected by filtration and washed with 1,4 dioxane thrice. The powder collected was then solvent exchanged with acetone 5-6 times and dried at 120 °C under vacuum for 12 h to get corresponding COF-Py powders.

Fabrication of 2D COF-Pa powders: 1,3,5-triformylphloroglucinol (Tp) (0.3 mmol), and p-phenylenediamine (Pa) (0.45 mmol) were dissolved in 3 mL (1:1) solvent mixture of 1,4-dioxane and mesitylene with 0.5 mL of 3 M acetic acid and added to a pyrex tube (o.d. × i.d. = 10 × 8 mm^2 and length 18 cm). This mixture was sonicated for 10 min to obtain a homogeneous dispersion, then dissolved after freezing at 77 K (liquid N_2 bath) and cycled three times for degassing. The tube was sealed off and heated at 120 °C for 72 h. A reddish-brown colored precipitate was collected by filtration and washed with dimethylacetamide thrice. The powder collected was then solvent exchanged with acetone 5-6 times and dried at 120 °C under vacuum for 12 h to get corresponding COF-Pa powders.

Ion permeation tests through 2D COF membranes: All permeation measurements were performed using the homemade H-Cell (Figure S2), which consists of two identical compartments separated by a membrane with an effective area of 1.766 cm^2. We take the single-ion permeation test of Li^+ as an example: 25 mL of 0.1 M LiCl aqueous solution and 25 mL of deionized water were added into the chambers, respectively. During the test, the COF side faced the feed solution chamber. Magmatic stirring (600 rpm) was applied to both sides to avoid concentration polarization. Inductively coupled plasma optical emission spectrometry (ICP-OES, OPTIMA 8000) determined the permeated cation concentrations. The data were recorded after the system reached a steady state. The test was operated at room temperature. The non-unary ion permeation tests were carried out using a similar method, but the feed side was filled with a mixture of testing target salts.

The ion permeation rate (J_i) could be calculated using the following equation

$$J_i = \frac{V \times C}{A \times \Delta t} \qquad (1)$$

where V is the effective volume of the solution on the permeated side, C is the detected concentration on the permeated side based on the ICP detection, A is the effective membrane area, and Δt is the permeation time. The ideal ion selectivity of multi-ions could be calculated using the following equation

$$\alpha = \frac{J_a}{J_b} \qquad (2)$$

where J_a and J_b are the ion permeation rates for components *a* and *b*, respectively.

Practical application performance of 2D COF membrane: With the assistance of the same H-Cell as mentioned, 25 mL of mixed aqueous solution (Li^+: Ni^{2+}: Co^{2+}: Mn^{2+} ration: 1: 0.8: 0.1: 0.1, Li^+ = 1 mol/L) was used as the feed solution, and the permeate side was filled with 25 mL of deionized water. Refreshing the feed solution and permeate solution after each test cycle. The permeation rate *(P*) of the cations (Li^+, Ni^{2+}, Co^{2+}, and Mn^{2+}) after each cycle was calculated using (1). The ideal ion selectivity of multi-ions could be calculated using (2). The actual separation factor of Li^+ over M^{2+} could be calculated using the following equation

$$S(Li^+, M^{2+}) = \frac{C_{Li^+,p}/C_{M^{2+},p}}{C_{Li^+,f}/C_{M^{2+},f}} \quad (3)$$

where $C_{M^{2+},p}$ (g·L^{-1}) and $C_{Li^+,p}$ (g·L^{-1}) refer to M^{2+} and Li^+ concentrations in the permeate solution, respectively; $C_{M^{2+},f}$ (mol·L^{-1}) and $C_{Li^+,f}$ (mol·L^{-1}) refer to M^{2+} and Li^+ concentrations in the feed solution, respectively.

Ion diffusion coefficient measurement: The diffusion coefficients of ions in 2D COF membranes could be calculated based on the classical diffusion equation shown below:

$$J = \frac{D}{d} \times \Delta c \times \frac{A_{eff}}{A} \quad (4)$$

where J (mmol m^{-2} h^{-1}) represents the permeation rate, which can be obtained by the concentration of ions in the permeate side during a certain time (20 min). *A* is the membrane area (7.065 cm^2). *D* is the diffusion coefficient of ions in the membrane, and *d* is the thickness of the membrane. Δc is the concentration gradient across the membrane (0.1 m in all experiments). The projected area of the free volume of Li^+ in the z-axis direction is considered as A_{eff}. The free volume of the simulation box is determined by the implemented tool 'gmx freevolume'. Specifically, a probe radius of 0.4 nm was set, which approximates the hydration radius of lithium ions. The program tries to insert such a probe into the simulation box, and a position is considered to be free if the distance between the probe and any atom is larger than the sum of the two van der Waals radii. For lithium, the estimated diffusion coefficient for 2D COF membranes had the same order of magnitude (≈ 1.029×10^{-5} cm^2 s^{-1} for Li$^+$), similar to that in the bulk solution. However, for divalent cations, the diffusion coefficient of those through 2D COF membranes has dropped by different orders of magnitudes. This significant decrease indicated a strong interaction between hydrated cations and the surface of the COF membrane.

Molecular dynamics (MD) simulations

Molecular dynamics simulations are performed with Gromacs 2019.6.[1] The simulation system contains three regions, i.e. the external region (pure water), the internal region (feed solution), and two COF regions separating the internal and external parts. Each COF region consists of five AA-stacked 2D COF-Pa/2D COF-Py layers. The feed solution consists of 5 Li$^+$, 5 Co^{2+}, 15 Cl$^-$, and about 3500 water molecules, corresponding to the catholic concentration at about 0.1 mol/L. Water is described by the OPC model.[2] Ions are parameterized as proposed by Merz. et al.[3, 4] 2D COF-Pa and 2D COF-Py are described by General Amber Force Field.[5] Lennard Jones (LJ) potential is used to describe the interatomic vdW interactions truncated at 1.2 nm. LJ parameters between unlike atom pairs are derived by Lorentz-Berthelot combination rules. Electrostatic interaction is calculated with the particle-mesh Ewald method. Energy minimization is performed to relax the initial configurations. Subsequently, 60-ns production runs are performed at 298.15 K and 1.0 bar. The equations of motion are integrated by the leapfrog algorithm. A time step of 1.0 fs is used. Three-dimensional periodic boundary conditions are applied during all simulations.

Density functional theory (DFT) calculations

One ion (Li$^+$, Mn^{2+}, Co^{2+}, Ni^{2+}) and 6 H_2O/(5 H_2O with Py) were severally put in a 15× 15 × 15 box to simulate the hydrated ion. Their binding energy was performed based on the Vienna ab initio simulation package (VASP). The Perdew-Burke-Ernzerhof with generalized gradient approximation (GGA) was adopted to describe the electron-electron interaction. An energy cutoff of 450 eV was used, and a k-point sampling set of 5 × 5 ×5 was tested to be converged.[6] The criterion for all structural optimizations was set to 10-5 eV for electronic energy convergence and Hellmann-

Feynman force less than 0.02 eV Å^{-1} for the ionic relaxation loop. The van der Waals dispersion forces were included using the zero damping DFT-D3 method of Grimme. The implicit solvent model, VASPsol, was applied to consider the effects between the solute and solvent on the activation energies.

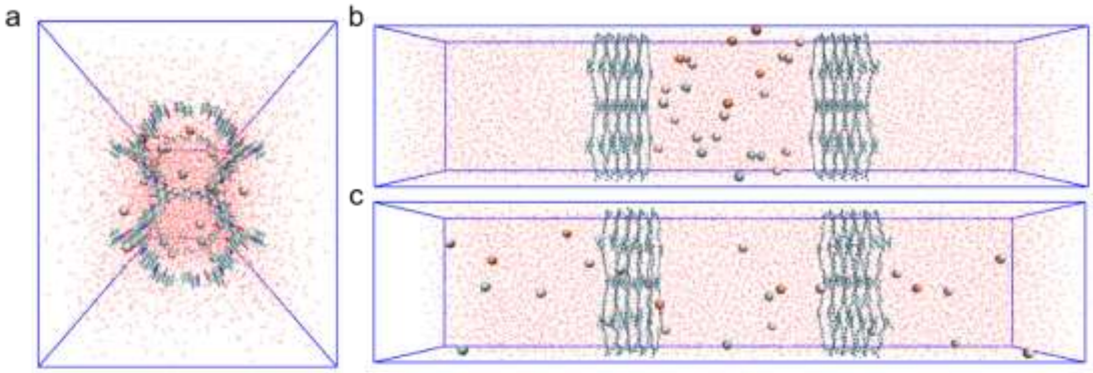

Figure S1. (a) The planform of the MD box to display the 2D COF-Pa layers. (b-c) MD simulation snapshots for ion diffusion through 2D COF-Pa layers at (b) 0 ns and (c) 50 ns. Analysis of the MD snapshots from a 50-ns simulation shows that both Li^+ and Co^{2+} can flee from the 2D COF-Pa layers without hindrance.

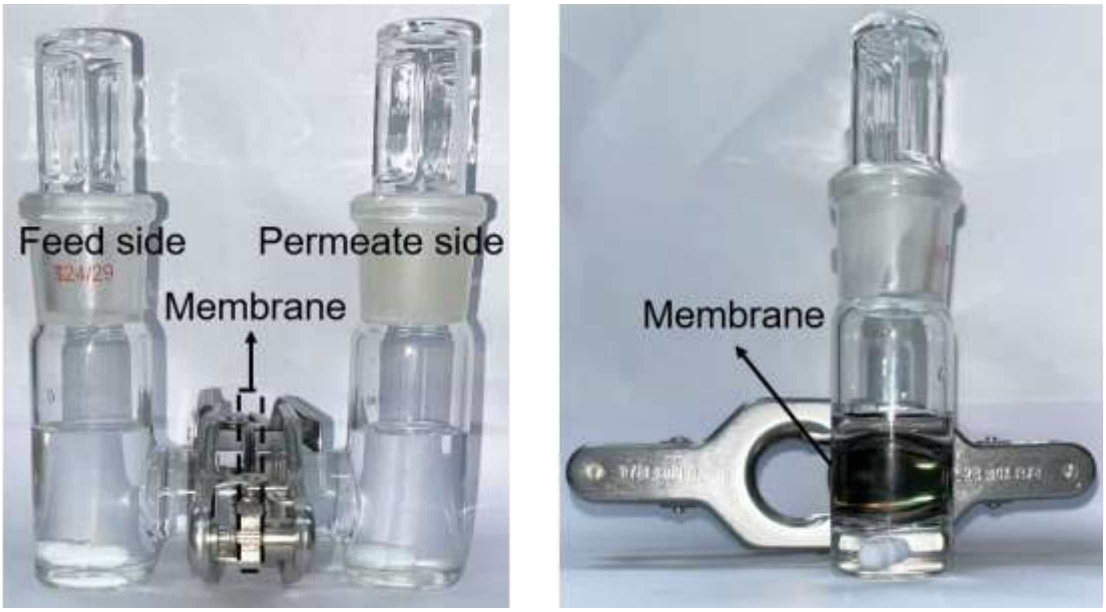

Figure S2. Digital photography of the homemade H-Cell devices applicable for ion-diffusion tests.

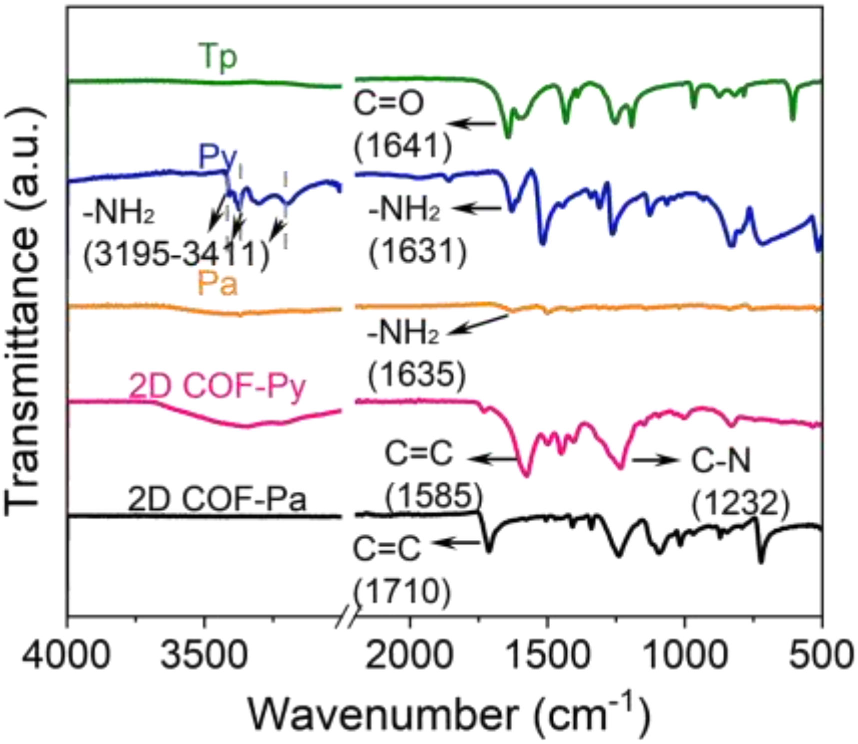

Figure S3. FTIR-ATR spectra of the monomers and 2D COF membranes.

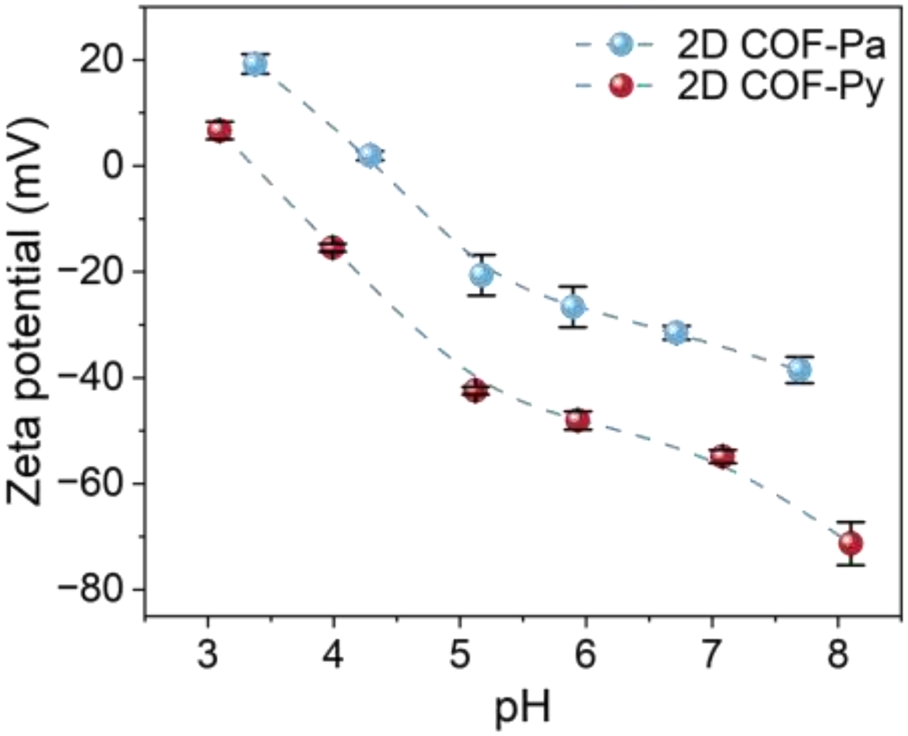

Figure S4. Zeta potential of 2D COF membranes as a function of pH values. In Figure S4, the 2D COF-Py membrane achieved the isoelectric point at ≈ 3.4, revealing that the membrane surface is neutral at a pH of approximately 3.4, negatively charged when pH exceeds 3.4 and positively charged when pH is below 3.4. Suffering from the lack of the negatively charged pyridine groups in the framework, the 2D COF-Pa membrane revealed the isoelectric point at ≈ 4.3, displaying a much lower negative charge than the 2D COF-Py ones regardless of solution conditions.

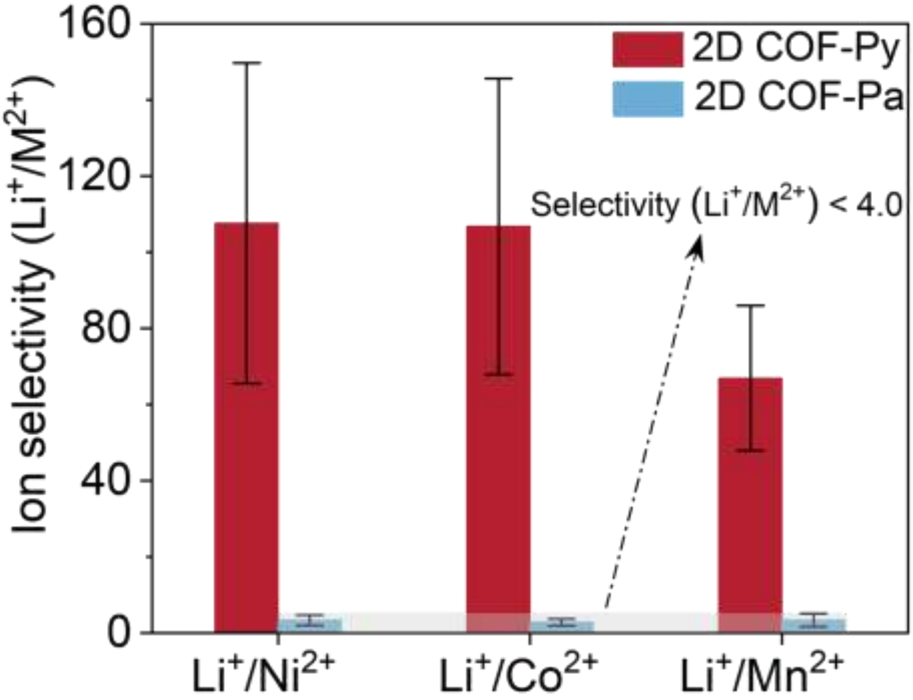

Figure S5. The ideal selectivity of Li^+/M^{2+} for 2D COF membranes. Feed solutions of 0.1 M XCl (X= Li, Ni, Co, and Mn) are used, while deionized (DI) water fills the permeate side, respectively.

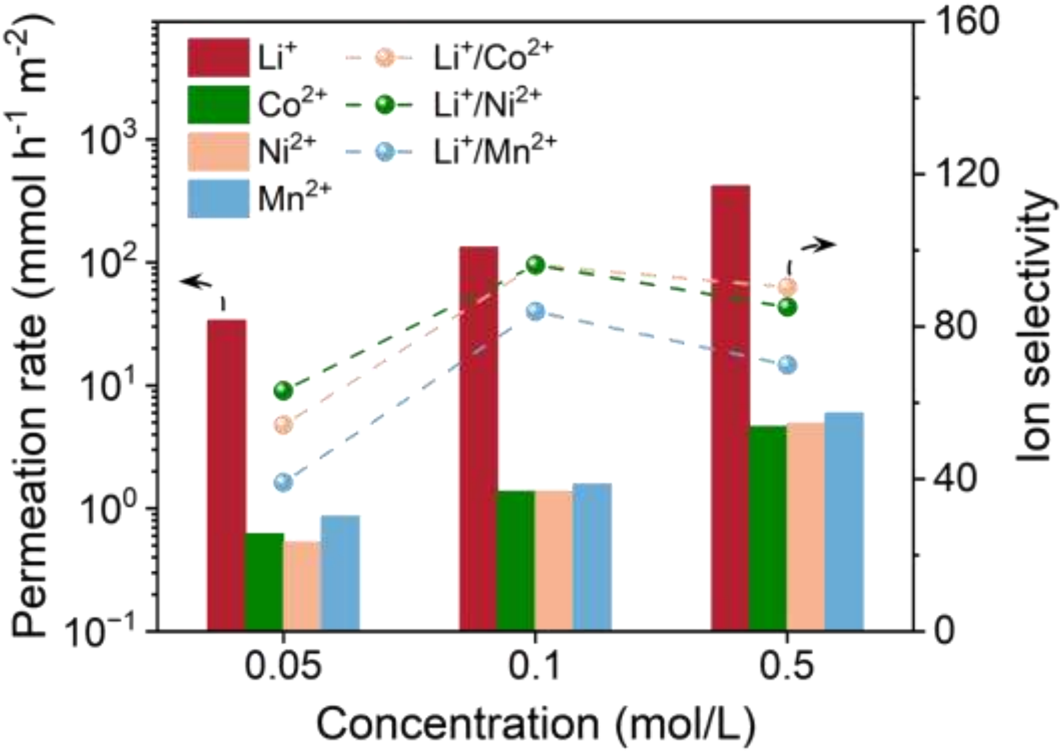

Figure S6. The ion permeation rates of Li^+ and M^{2+}, and the corresponding ion selectivity (Li^+/M^{2+}) for 2D COF-Py membranes under different concentration gradients. There exists a positive relevance between divalent cations' penetration rates and the concentration gradient. The divalent cations' permeation rates slightly rise along with the increase of concentration gradient. However, the Li^+ permeation rates suddenly surged when the concentration changed from 0.1 to 0.5 M. Consequently, the Li^+/M^{2+} selectivity increased first upon changing the concentration from 0.05 to 0.1 M and underwent a slight decline by further raising the concentration to 0.5 M.

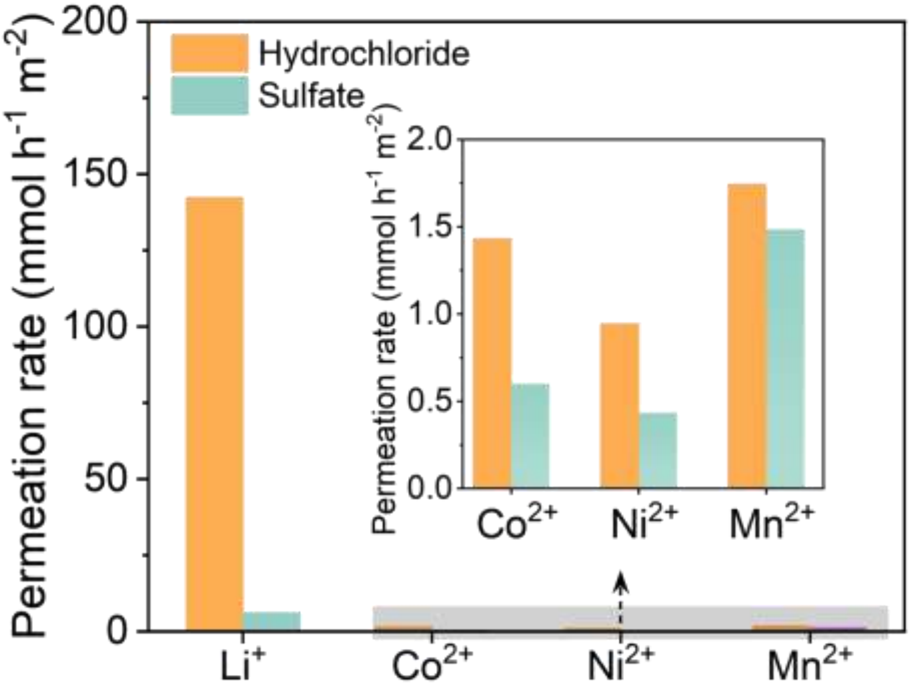

Figure S7. Comparison of permeation rate between sulfate solution and chloride solution of 2D COF-Py membrane. Under sulfate anion conditions, the permeation rate of cations decreases overall, but the Li^+ permeation rate is still significantly higher than divalent ones.

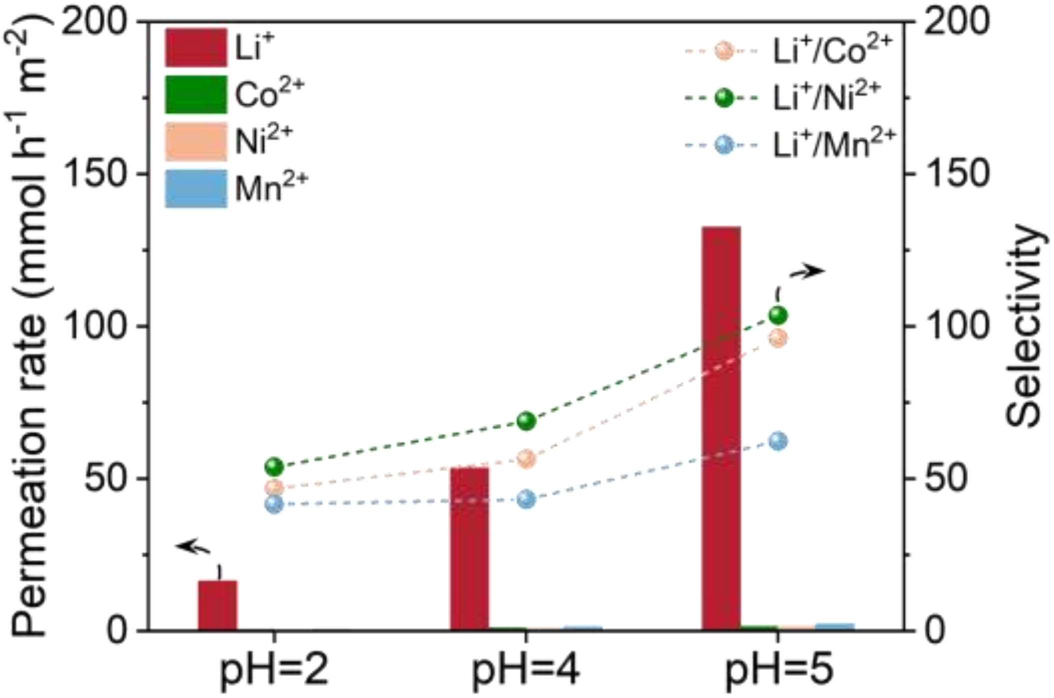

Figure S8. Comparison of ion separation performance of 2D COF-Py membrane under different pH environments. At lower pH values, there is a significant decrease in ion permeation rate and a noticeable decline in ion selectivity.

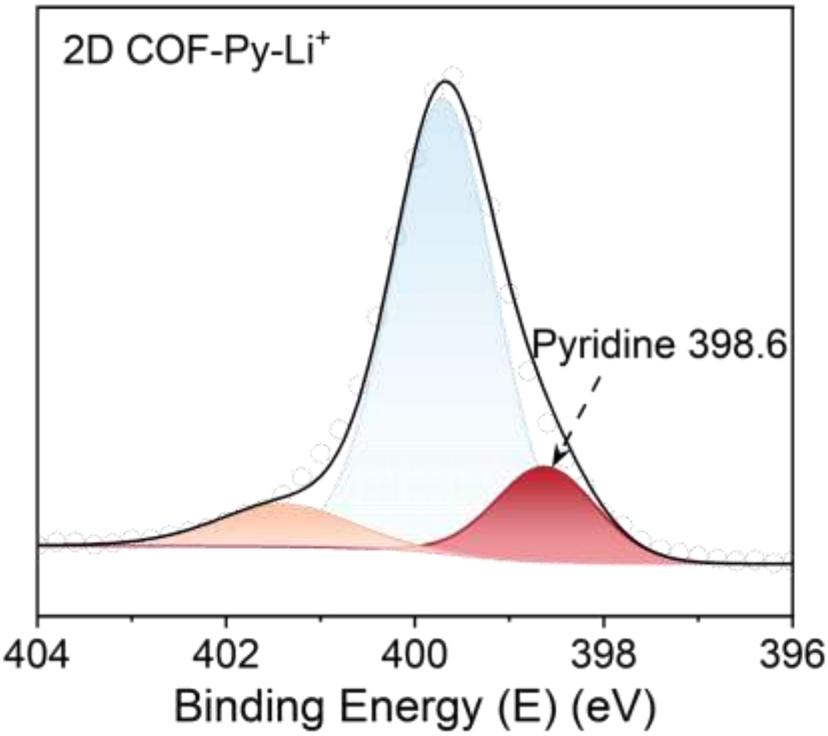

Figure S9. N1s XPS spectra of 2D COF-Py membrane immersed in LiCl solution. The pyridine N (-C_5H_5N) peak at 398.6 eV was observed with negligible displacement compared with the original 2D COF-Py membrane, showing little coordination interaction between Li^+ and pyridine binding site.

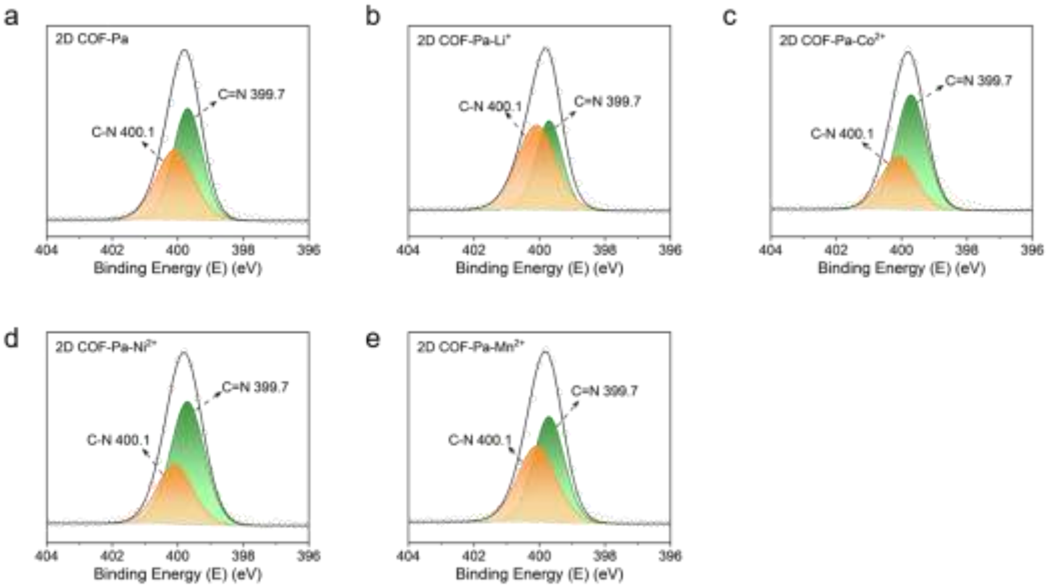

Figure S10. N1s XPS spectra of 2D COF-Pa membrane immersed in different solutions. Two peaks at 399.7 and 401.1 eV are characteristic N1s signals for the C=N (green), and C-NH (orange), respectively.[7, 8] No significant shift occurred after solution treatment, suggesting the absence of strong coordination interaction between the divalent cations and 2D COF-Pa membrane. Besides, this result indicates that these divalent cations cannot form the complexation-like interaction with other nitrogen functional groups (e.g. -NH-) anchored on the COF-Pa framework.

Table S1. Monovalent cation/divalent cation selectivity (Li^+/M^{2+}) and ion permeation rate (Li^+) were revealed by different artificial channels (nanomaterial membranes) measured in the binary ion system.

Membrane Material	Separation method	Concentration	Li^+ flux (mmol m^{-2} h^{-1})	Selectivity (Li^+/M^{2+})	Ref
2D COF-Py membranes	**diffusion**	**0.1 M LiCl; 0.1 M $CoCl_2$ 0.1 M $NiCl_2$ 0.1 M $MnCl_2$**	**32.22 33.39 34.24**	**53.45 64.96 47.28**	**This work**
MOF@PVC membranes	diffusion	0.1 M LiCl; 0.1 M $MgCl_2$	1.19	4.73	9
LDH laminar membrane	diffusion	0.1 M LiCl; 0.1 M $MgCl_2$	7	6	10
HMO@AEMs membranes	diffusion	1 M LiCl; 1 M $MgCl_2$	1100	9.17	11
2D MMT membranes	diffusion	0.1 M LiCl; 0.1 M $MgCl_2$	600	9.2	12
UIO-66 membranes	diffusion	0.1 M LiCl; 0.1 M $MgCl_2$	720	12.07	13
VmNS2-6 membrane	diffusion	0.2 M LiCl; 0.2 M $MgCl_2$	140	15,6	14
GO membranes	diffusion	0.25 M LiCl; 0.25 M $MgCl_2$	70	16.8	15
i-CMP membranes	diffusion	0.1 M LiCl; 0.1 M $MgCl_2$	32.6	17	16
trans-COF-AzoSO$_3$H-50 membrane	diffusion	0.1 M LiCl; 0.1 M $MgCl_2$	20	36.6	17
TpEBr COF membrane	diffusion	0.2 M LiCl; 0.2 M $MgCl_2$	50	41.1	18

Reference

1. M. Abraham, T. Murtola, R. Schulz, S. Páll, J. Smith, B. Hess and E. Lindahl, GROMACS: High performance molecular simulations through multi-level parallelism from laptops to supercomputers, *SoftwareX*, 2015, **1**, 19-25.
2. S. Izadi, R. Anandakrishnan and A. Onufriev, Building water models: a different approach, *J. Phys. Chem. Lett.*, 2014, **5**, 3863-3871.
3. A. Sengupta, Z. Li, L. Song, P. Li and K. M. Jr, Parameterization of monovalent ions for the OPC3, OPC, TIP3P-FB, and TIP4P-FB water models, *J. Chem Inf. Model.*, 2021, **61**, 869-880.
4. Z. Li, L. Song, P. Li and K. M. Jr, Systematic parametrization of divalent metal ions for the OPC3, OPC, TIP3P-FB, and TIP4P-FB water models, *J. Chem. Theory Comput.*, 2020, **16**, 4429-4442.
5. J. Wang, R. Wolf, J. Caldwell and P. Kollman, Development and testing of a general amber force field, *J. Comput. Chem.*, 2004, **25**, 1157-1174.
6. S. Chill, J. Stevenson, V. Ruehle, C. Shang, P. Xiao, J. Farrell, D. Wales and G. Henkelman, Benchmarks for characterization of minima, transition states, and pathways in atomic, molecular, and condensed matter systems, *J. Chem. Theory Comput.*, 2014, **10**, 5476-5482.
7. X. Zhong, Z. Lu, W. Liang and B. Hu, The magnetic covalent organic framework as a platform for high-performance extraction of Cr (VI) and bisphenol a from aqueous solution, *J. Hazard. Mater.*, 2020, **393**, 122353.
8. R. Wen, Y. Li, M. Zhang, X. Guo, X. Li, X. Li, J. Han, S. Hu, W. Tan and L. Ma, Graphene-synergized 2D covalent organic framework for adsorption: A mutual promotion strategy to achieve stabilization and functionalization simultaneously, *J. Hazard. Mater.*, 2018, **358**, 273-285.
9. C. Zhang, Y. Mu, W. Zhang, S. Zhao and Y. Wang, PVC-based hybrid membranes containing metal-organic frameworks for Li^{+}/Mg^{2+} separation, *J. Membr. Sci.*, 2020, **596**, 117724.
10. B. Li, J. Peng, M. Li, Z. Yang, J. Lu and J. Han, Facile synthesis and exfoliation of micro-sized LDH to fabricate 2D membranes towards Mg/Li separation, *AICHE J.*, 2023, ***69***, 18212.
11. G. Luo, Y. Wu, X. Zeng, W. Zhou, P. Wang and W. Zhang, Lithium-Ion-Sieve-Embedded Hybrid Membranes for Anion-Exchange- and Cation-Concentration-Driven Li/Mg Separation, *ACS Appl. Mater. Interfaces*, 2024, DOI: 10.1021/acsami.3c19100, 3c19100.
12. T. Wen, Y. Zhao, X. Wang, L. Chen, R. Gao, S. Wang and T. Zhang, Efficient and ultrafast separation of Li^{+} and Mg^{2+} by the porous two-dimensional nanochannel of perm-selective montmorillonite membrane, *Chem. Eng. J.*, 2023, ***475***, 146101.
13. X. Zeng, L. Xu, T. Deng, Y. Wang, W. Xu and W. Zhang, Anionic MOFs Embedded in Anion-Exchange Membranes for the Separation of Lithium/Magnesium Cations, *ACS Sustain. Chem. Eng.*, 2023, ***11***, 12877-12887.
14. L. Dai, S. Pang, S. Li, Z. Yi, K. Qu, Y. Wang, Y. Wu, S. Li, L. Lei, K. Huang, X. Guo and Z. Xu, Freestanding two-dimensional nanofluidic membranes modulated by

zwitterionic polyelectrolyte for mono-/di-valent ions selectivity transport, *J. Membr. Sci.*, 2023, ***677***, 121621.

15. W. Zhang, Q. Huang, S. Liu, M. Zhang, G. Liu, Z. Ma and W. Jin, Graphene oxide membrane regulated by surface charges and interlayer channels for selective transport of monovalent ions over divalent ions, *Sep. Purif. Technol.*, 2022, ***291***, 120938.
16. Z. Zhou, D. B. Shinde, D. Guo, L. Cao, R. A. Nuaimi, Y. Zhang, L. R. Enakonda and Z. Lai, Flexible Ionic Conjugated Microporous Polymer Membranes for Fast and Selective Ion Transport, *Adv. Funct. Mater.*, 2021, ***32***, 2108672.
17. L. Ren, J. Chen, J. Han, J. Liang and H. Wu, Biomimetic construction of smart nanochannels in covalent organic framework membranes for efficient ion separation, *Chem. Eng. J.*, 2024, **482**, 148907.
18. R. Wang, L. Ding, J. Xue, H. Wu, C. Cai, Z. Qiao, J. Caro and H. Wang, Engineering of Covalent Organic Framework Nanosheet Membranes for Fast and Efficient Ion Sieving: Charge-Induced Cation Confined Transport, *Small Methods*, 2024, 2401111.